

Comparisons of aerosol optical properties derived from Sun photometry to estimates inferred from surface measurements in Big Bend National Park, Texas

J.L. Hand^{a,*}, S.M. Kreidenweis^b, J. Slusser^c, G. Scott^c

^a*Cooperative Institute for Research in the Atmosphere, Colorado State University, 1375 Campus Delivery, Fort Collins, Colorado 80523, USA*

^b*Department of Atmospheric Science, Colorado State University, Fort Collins, Colorado 80523, USA*

^c*UVB Monitoring Program, Natural Resource Ecology Laboratory, Colorado State University, Fort Collins, Colorado 80523, USA*

Received 5 May 2004; accepted 30 August 2004

Abstract

As a part of the Big Bend Regional Aerosol and Visibility Observational Study (BRAVO, July–October 1999), aerosol physical, optical and chemical properties were measured continuously in an effort to characterize visibility in Big Bend National Park. Surface-based estimates of aerosol extinction coefficients derived from size distribution data were compared to aerosol optical properties retrieved independently from ground-based remote sensing measurements from the United States Department of Agriculture (USDA) UVB radiometer network site. Comparisons suggested that for the majority of the study, surface visibility was a good indicator of the column aerosol optical depth, with a correlation coefficient of $r^2 = 0.77$. The average (and one standard deviation) aerosol optical depth from the USDA network was 0.13 ± 0.06 at a wavelength of 500 nm. Ångström wavelength exponents were computed for both data sets to characterize the spectral variations of aerosol optical properties over the wavelength range of 415–860 nm. Variations in Ångström exponents corresponded to changing aerosol properties as seen in the ground-based composition and size distribution data sets. The average Ångström exponent from in situ measurements was 1.5 ± 0.4 compared to column estimates of 1.3 ± 0.4 . The root mean square of the difference between the estimates of Ångström exponents was 0.20 (~12%) and on average the estimates were highly correlated ($r^2 = 0.89$). Aerosol optical depths and ambient surface aerosol extinction coefficients were positively correlated with PM_{2.5} sulfate mass concentrations ($r^2 = 0.68$ and $r^2 = 0.79$, respectively), suggesting that sulfate aerosols were a major contributor to visibility degradation and column aerosol loading during the study.

© 2004 Elsevier Ltd. All rights reserved.

Keywords: Ångström exponent; Dust; Sulfate aerosols; Extinction coefficient; Aerosol optical depth; Aerosol optical properties; Visibility; Remote sensing; Sun photometer

1. Introduction

The effects of aerosols represent one of the largest uncertainties in predicted climate change (Haywood and Boucher, 2000). The role of aerosol direct forcing on climate may be similar in magnitude to the effects of

*Corresponding author. Tel.: +970 491 3699;
fax: +970 491 8598.

E-mail address: hand@cira.colostate.edu (J.L. Hand).

greenhouse gases and can range from cooling to warming depending on the aerosol composition (IPCC, 2001). Clearly, the aerosol effect is important for understanding current and future climate, and knowledge of aerosol radiative properties is critical. Studies that measure the physical, chemical and optical properties of aerosols are necessary to improve understanding of the complex nature of atmospheric aerosols and their effects on climate change.

Estimates of direct forcing have typically relied on surface measurements of aerosol radiative properties with the assumption that the properties at the surface represent those of a well-mixed column (Charlson et al., 1992; IPCC, 2001). Whether this assumption is appropriate in general has yet to be shown systematically. One method used to test this assumption is to perform closure experiments by comparing aerosol optical depths, τ_{aer} , from surface-based remote sensing with the vertically integrated aerosol extinction coefficient, b_{ext} , measured at the surface. Bergin et al. (2000) reviewed several such experiments and noted that some of the inherent difficulties included differences in relative humidity (RH) effects on aerosol optical properties measured with a nephelometer at the surface compared to the column-based ambient optical properties. Comparisons of aerosol optical depths derived from airborne and ground measurements at the Southern Great Plains (SGP) Atmospheric Radiation Measurement (ARM) site by Kato et al. (2000) suggested that the fraction of aerosol optical depth due to scattering by particles in the boundary layer to that of the entire column is approximately 0.4. Corbin et al. (2002) found only weak correlations between aerosol optical depth from remote-sensing data and ground-based composition data at urban locations, probably because of the lack of aerosol vertical profile data and RH information. Recent work by Andrews et al. (2004) suggests that long-term ground-based measurements at the SGP site are representative of column aerosol properties but may not capture the day-to-day variability in the column. These varying results for different periods and locations suggest that more closure experiments are needed for understanding whether systematic relationships exist between ground-based and column measurements.

A similar closure experiment was performed with surface-based measurements of aerosol optical properties during the Big Bend Regional Aerosol and Visibility Observational (BRAVO) Study. One goal of the BRAVO study was to characterize visibility in Big Bend National Park, located in a remote region of southwest Texas, on the border with Mexico. Despite this remote location, Big Bend National Park tends to have some of the poorest visibility of any Class 1 monitored area in the western United States (Gebhart et al., 2001). The BRAVO site was located on the eastern side of the park at an elevation of 1075 m (29.3°N, 103.18°W). Contin-

uous aerosol measurements were performed to characterize the physico-chemical and optical properties of accumulation and coarse mode particles (Hand et al., 2002; Lee et al., 2004). No data were available to infer the vertical distribution of aerosol properties or mixing layer depths from the surface-based in situ data. Column aerosol properties were derived from solar irradiance measurements from a multifilter rotating shadowband radiometer (MFRSR) operating independently as a part of the United States Department of Agriculture (USDA) UVB network (Bigelow et al., 1998) at a site located in Big Bend National Park at an elevation of 670 m (29.1°N, 103.5°W). The USDA site was approximately 30 miles southwest from the BRAVO study site and separated from it by the Chisos Mountain range. Spectral parameters were estimated from both the surface and column measurements. Ångström wavelength exponents were calculated from extinction coefficients derived from size distribution measurements and from aerosol optical depths from the visible radiometer over the wavelength range of 415–860 nm.

2. Experimental methods

2.1. USDA UVB network

In 1992 the USDA established a UVB radiation monitoring network to quantify the spatial and temporal distribution of UVB radiation and its impact on agricultural production in the US (Bigelow et al., 1998). Both UV and visible MFRSR are operated in Big Bend National Park, but data from the visible MFRSR (VIS-MFRSR) are used in this paper (Harrison et al., 1994). The VIS-MFRSR measures total horizontal, diffuse and direct normal irradiance at five wavelength channels ($\lambda = 415, 500, 610, 665, 860$ nm) every 15 s and reports 3-min averaged data.

The Langley short method as applied to the Beer–Lambert law was used for instrument calibration (Slusser et al., 2000; Harrison and Michalsky, 1994) but not for cloud removal. In order to obtain aerosol optical depth from this measurement, the contributions from Rayleigh and gaseous optical depths were removed. Rayleigh optical depth is wavelength and pressure dependent and was computed according to the site elevation and channel wavelengths following Hansen and Travis (1974). The gaseous optical depth was attributed to ozone and was computed using monthly averaged column ozone estimates from the total ozone mapping spectrometer (TOMS, Herman et al., 1999) and weighted ozone cross sections (Bigelow et al., 1998). Monthly averaged values of column ozone for July, August, September and October at Big Bend National Park were 297 DU, 297 DU, 281 DU and 276 DU, respectively. Schmid et al. (1999) derived aerosol optical

depth in a similar manner from several Sun photometers located at the SGP facility and found a typical accuracy of 0.026, with a root mean square (RMS) of 0.015 for these types of measurements. McArthur et al. (2003) reported an RMS of 0.0069 for aerosol optical depths ($\lambda = 500$) from direct Sun-pointing instruments operated during a 3-month study.

Cloud-contaminated data were removed following the method of Smirnov et al. (2000) for the AERONET database. Although the method was developed specifically for the Sun photometers in the AERONET network (Holben et al., 1998), it was applied successfully to the 3-min data retrieved from the UVB Sun photometers to remove data during periods contaminated by clouds. No restrictions of data based on low Ångström exponents were imposed because it was apparent from size distribution data that periods with significant coarse particle concentrations occurred that would result in lower values of Ångström exponents. Instead, time periods when rapid increases in aerosol optical depth coincided with rapid decreases and very low values of Ångström wavelength exponents (~ 0) suggested the presence of cirrus clouds and were removed (Smirnov et al., 2000). Removal of data from these periods may have resulted in removing some valid aerosol data instead of cloud-contaminated periods.

2.2. Surface-based aerosol measurements

Dry aerosol size distributions ($0.05 < D_p < 20 \mu\text{m}$) were measured continuously during the BRAVO study in order to characterize the accumulation and coarse mode particles. Dry measurements were performed to avoid uncertain particle sizing from changing RH in the ambient and sampled air. Number concentrations were measured as a function of size using a differential mobility analyzer, optical particle counter and aerodynamic particle sizer. The data from each instrument were expressed as a complete size distribution using the method presented in Hand and Kreidenweis (2002). This method allowed for the retrieval of particle real refractive index and effective density. Aerosol $\text{PM}_{2.5}$ concentrations were compiled from a variety of filter-based and continuous measurements, and included estimates of ammoniated sulfate, nitrate, organic carbon (OC), elemental carbon and mineral soil concentrations (Lee et al., 2004). Nitrate was assumed to be in the form of NaNO_3 , rather than NH_4NO_3 , as sulfate was not fully neutralized on average and size-fractionated impactor samples demonstrated that nitrate was typically associated with coarse mode particles (Lee et al., 2004). OC mass concentrations were derived from TOR combustion analyses (Chow et al., 1993). Black carbon (BC) mass concentrations were measured with a McGee Scientific aethalometer. Mineral soil mass concentrations were computed following the IMPROVE soil

formula as a sum of oxides of aluminum, silicon, calcium, iron and titanium (Malm et al., 1994). Soil, OC, BC and nitrate mass concentrations were 20%, 22%, 2% and 4% of the study-averaged $\text{PM}_{2.5}$ aerosol mass concentrations, respectively, and ammoniated sulfate concentrations dominated the fine mode aerosol composition (53% by mass, on average) (Lee et al., 2004).

The hourly averaged dry size distributions, adjusted for water content at ambient RH (Hand et al., 2000), were used to compute b_{ext} . Aerosol water content was estimated from hourly averaged surface RH measurements and the theoretical water content of the metastable ammoniated sulfate compound (Tang, 1996), which ranged from fully ammoniated sulfate to compositions near sulfuric acid. The study average aerosol ammonium to sulfate molar ratio was 1.53 ± 0.3 (Lee et al., 2004), suggesting an acidic aerosol on average. Ammoniated sulfate species were the only species assumed to be hygroscopic during BRAVO, as demonstrated by Malm et al. (2003), and the non-hygroscopic species (dust, organic and elemental carbon) did not contribute to particle growth (Malm and Kreidenweis, 1997). The average surface relative humidity observed during BRAVO was $46 \pm 18\%$. The b_{ext} calculations accounted for variations in particle refractive index due to the addition of water, increased aerosol mass with added water, and changes in the aerosol size distributions due to particle growth by water uptake. Eq. (1) was used to compute the ambient light extinction coefficient from measured dry volume distributions and diameters:

$$b_{\text{ext}} = \int \frac{3}{2} \frac{Q_{\text{ext,amb}}}{D_{\text{p,dry}}} [f(\text{RH})]^2 \frac{dV_{\text{dry}}}{d \log D_p} d \log D_p, \quad (1)$$

where $f(\text{RH})$ is the diameter growth factor derived from estimates of aerosol water content and $Q_{\text{ext,amb}}$ is the Mie extinction efficiency computed with ambient diameters $D_{\text{p,amb}} = f(\text{RH})D_{\text{p,dry}}$ and complex refractive indices adjusted for water content. The integral in Eq. (1) was performed over the full size distribution, including both the fine and coarse particle modes ($D_p = 0.05 - 20 \mu\text{m}$). The real part of the dry complex refractive index ($n = m + ki$) was obtained from the method described by Hand and Kreidenweis (2002) that aligned size distributions from a differential mobility analyzer and an optical particle counter in their overlapping size range. The sizing by the optical particle counter depends on refractive index; therefore, the value that results in the best agreement in size distributions between the instruments is assumed to correspond to the particle refractive index. The resulting average (\pm one standard deviation) dry refractive index of $m = 1.566 \pm 0.012$ agreed within uncertainties to estimates derived from bulk composition data using a volume-weighted method (Hasan and Dzubay, 1983; Ouimette and Flagan, 1982). Hourly averaged BC

concentrations were used in a volume-weighted method to estimate the magnitude of the absorbing part, which was a study average of $k = 0.014 \pm 0.004$. The volume-weighted method is shown in Eqs. (2) and (3). The mean complex refractive index ($\bar{n} = \bar{m} + \bar{k}i$) is computed with the real refractive index for species j (m_j), the mass fraction for species j (X_j) and the species density (ρ_j , g cm^{-3}). The mean imaginary part of the complex refractive index is computed using the value corresponding to each species (k_j):

$$\bar{n} = \bar{\rho} \sum_j \frac{X_j m_j}{\rho_j} + \bar{\rho} \sum_j \frac{X_j k_j}{\rho_j} i. \quad (2)$$

The mean density $\bar{\rho}$ is computed with

$$\bar{\rho}^{-1} = \sum_j \frac{X_j}{\rho_j}. \quad (3)$$

Estimates of b_{ext} were computed for five visible wavelengths (415, 500, 610, 665 and 860 nm). Comparisons of dry particle light-scattering coefficients derived from size distributions (following Eq. (1)) with values measured using a nephelometer were shown by Hand et al. (2002) to result in an $\sim 30\%$ bias with higher values corresponding to estimates derived from size distributions. This bias suggested that the theoretical loss calculations applied to the size distribution data may be too large. Hand et al. (2002) also found that using refractive indices derived from a volume-weighted method resulted in only a 3% difference in computed light-scattering coefficients.

3. Ångström exponent

The spectral dependence of τ_{aer} is important for modeling the radiative effects of aerosols on the Earth/atmosphere system and is related to the aerosol size distribution. To quantify the spectral dependence of τ_{aer} , Ångström's (1929) empirical equation was used:

$$\tau_{\text{aer}} = \beta \lambda^{-\alpha}. \quad (4)$$

The Ångström turbidity coefficient is denoted β , the wavelength (λ) is in micrometers and α is the Ångström wavelength exponent. Ratioing Eq. (4) at two wavelengths and taking the logarithm gives

$$\alpha = -\frac{d \ln(\tau_{\text{aer}})}{d \ln(\lambda)}. \quad (5)$$

Higher values ($\alpha > 2.0$) are typically observed for accumulation mode particles (Reid et al., 1999; Eck et al., 1999; Nakajima and Higurashi, 1998) and lower values (α near 0) have been observed for Saharan dust episodes and coarse mode particles (Eck et al., 1999; Smirnov et al., 1998). In this work, the Ångström wavelength exponent was computed using a least-squares fit of $\ln(\tau_{\text{aer}})$ versus $\ln(\lambda)$ for the USDA measurements (α_{col}) and a least-squares fit of $\ln(b_{\text{ext}})$ versus $\ln(\lambda)$ for the surface measurements (α_{sfc}), over the full range of visible wavelengths from the radiometer measurements ($415 \leq \lambda \leq 860$ nm). The range of values of Ångström exponent will depend on the number and values of wavelengths used in Eq. (5).

4. Results and discussion

A time series plot of hourly averaged ambient b_{ext} , and τ_{aer} ($\lambda = 500$ nm) derived from the Sun photometer is presented in Fig. 1. Experimental uncertainties in b_{ext} at $\lambda = 500$ nm are on the order of $\pm 10\%$. Experimental uncertainties in τ_{aer} are ± 0.01 at $\lambda = 500$ nm, and the minimum detection limit at this wavelength was $\tau_{\text{aer}} = 0.02$. The correlation coefficient between surface and column estimates for the study period was $r^2 = 0.77$. Monthly correlation coefficients were highest for September and October ($r^2 > 0.78$) when some of the largest values of b_{ext} and τ_{aer} were observed. The lowest monthly correlation coefficient was observed in July ($r^2 = 0.24$). Further inspection revealed that data from DOY 193 (12 July) were the cause of the weak correlation between b_{ext} and τ_{aer} in July. Removing this day from the comparison increased the July correlation

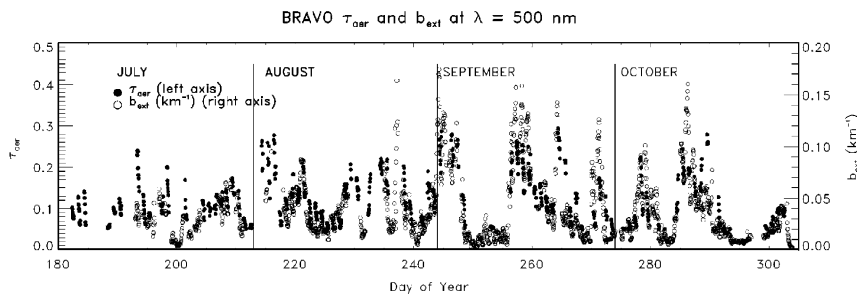


Fig. 1. Time series plot of column aerosol optical depth τ_{aer} derived from the USDA network on the left axis, compared with surface estimates of ambient b_{ext} (km^{-1}) from measurements of aerosol size distributions on the right axis. Both estimates correspond to a wavelength of 500 nm.

between b_{ext} and τ_{aer} to $r^2 = 0.68$. On this day, τ_{aer} nearly doubled in magnitude compared to DOY 192 and DOY 194. Surface b_{ext} data were not available on DOY 192 and DOY 194 so it was not possible to examine changes in the surface aerosol properties during the same period. Horizontal spatial variability due to differences in site locations, variations in vertical distribution of RH or aerosol extinction coefficients, or inefficient cloud removal could contribute to differences observed on DOY 193. Generally, the high correlations between surface and column measurements in Big Bend National Park during the study period are not surprising given that the dry surface conditions and strong afternoon sensible heat flux can result in deep mixed layers. No frontal inversions are expected in this region during the time period of the study, but elevated inversions may exist due to heated air from elevated regions of Mexico being advected into the area (D. Johnson, personal communication).

Timelines of Ångström wavelength exponents derived from both methods are shown in Fig. 2. The overall average value and one standard deviation of the Ångström exponent from the surface-based measurements was $\alpha_{\text{sfc}} = 1.5 \pm 0.4$ and from the USDA column-based measurement it was $\alpha_{\text{col}} = 1.3 \pm 0.4$. Typical uncertainties in column and surface Ångström exponents are approximately 0.2, and were computed following Kato et al. (2000). High correlations between the two estimates were observed for each month and the overall correlation coefficient was $r^2 = 0.89$. The highest monthly correlation coefficient was found in July ($r^2 = 0.97$) compared to the lowest in September ($r^2 = 0.53$). Larger percent differences ($>40\%$) between column and surface Ångström exponents typically coincided with cleaner periods (e.g. DOY 227, 253, 268, 282, 292–293) and contributed to the poorer correlations later in the study. These discrepancies are likely due to uncertainties in the MFRSR retrievals for low values of τ_{aer} . The overall percent difference between the two estimates of Ångström exponents was 12% with an RMS of 0.2.

Principal component analysis was used to investigate relationships between aerosol physical, chemical and optical properties (Henry and Hidy, 1979). The composition data incorporated in the analysis were the 24-h $\text{PM}_{2.5}$ compositions (see Section 2.2), and included ammoniated sulfate, sodium nitrate, organic and elemental carbon, and mineral soil. The optical and physical properties incorporated into the analysis were b_{ext} , τ_{aer} , Ångström exponents from the surface and remote-sensing measurements, and the fraction of the total volume concentration that is associated with coarse mode particles ($V_{\text{coarse}}/V_{\text{total}}$) determined from size distribution data (Hand et al., 2002). The composition, optical and physical aerosol data were loaded onto principal components based on the calculation of eigenvectors of the correlation coefficient matrix of the centered and scaled data. Three principal components that accounted for a majority of the variation (87%) in the data matrix were subjected to varimax rotation. Temporal trends were investigated by using the principal component scores from the rotated eigenvectors. Table 1 lists the resulting eigenvalues and corresponding percent variance explained.

The highest loadings for factor 1 (explaining 50% of the variance) included b_{ext} , τ_{aer} and ammoniated sulfate, consistent with high correlations observed between ammoniated sulfate and both τ_{aer} and b_{ext} for the study period ($r^2 = 0.68$ and $r^2 = 0.79$, respectively). Hering et al. (2003) also showed a strong relationship between measured and computed light-scattering coefficients, accumulation mode volume concentrations and sulfate mass measurements during BRAVO. This factor suggests that sulfate aerosols were responsible for decreased visibility as well as higher optical depths during the study. The scores for this factor were highest on DOY 244, 256–259, 278 and 285, corresponding to days when b_{ext} and τ_{aer} were high (Fig. 1); high accumulation mode volume concentrations and sulfate mass concentrations were also seen on those days (Hand et al., 2002; Hering et al., 2003).

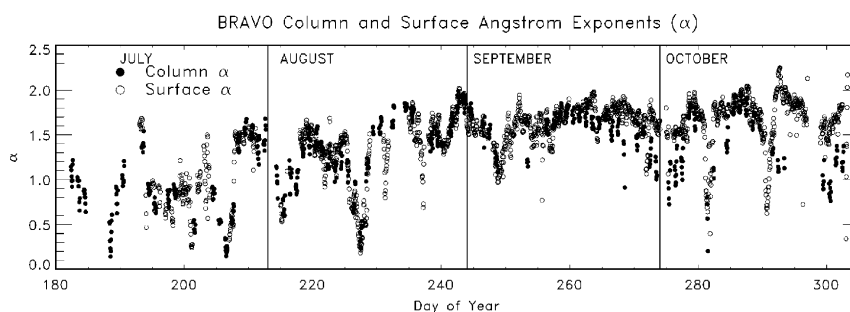


Fig. 2. Time series plot of Ångström wavelength exponents computed over the wavelength range of 415–860 nm. The column estimates (α_{col}) were derived from the spectral variation of aerosol optical depth (τ_{aer}) derived from the USDA network, and the surface estimates (α_{sfc}) were derived from surface estimates of ambient b_{ext} (km^{-1}).

Table 1
Eigenvalues and variance explained by each eigenvector

Eigenvalue	% Variance explained
5.05	50.5
2.51	25.1
1.14	11.4
0.34	3.4
0.27	2.7
0.22	2.2
0.20	2.0
0.12	1.1
0.09	0.9
0.07	0.7

Column estimates of Ångström exponents were weakly loaded onto factor 1 also. Periods with large Ångström exponents often corresponded to high sulfate fine mass concentrations (mostly during September and October; Lee et al., 2004) and also to higher values of b_{ext} and τ_{aer} . Transport during periods in which the particle size distribution was dominated by accumulation mode particles was typically from the Texas/Mexico border, eastern Texas and the eastern US (Hand et al., 2002). Monthly average values of α_{sfc} in September and October were 1.62 ± 0.19 and 1.7 ± 0.3 , respectively. The monthly average values of α_{col} in September and October were 1.6 ± 0.2 and 1.4 ± 0.4 , respectively. Figs. 3a and b explore the relationship between the fraction of aerosol volume contained in the accumulation mode and the column and surface Ångström exponents, respectively. More data are shown in Fig. 3b because values of α_{sfc} were computed for day and night, whereas the retrievals of α_{col} were only during daytime. The relationship between Ångström exponent and volume ratios is similar for both methods: when total volume concentrations were dominated by accumulation mode particles, the Ångström exponent increased, consistent with the presence of smaller, accumulation mode particles that have a stronger spectral dependence. Similar relationships were observed by Andreae et al. (2002) for a remote desert site in Israel.

Variables loaded strongly on factor 2 (25% of the variance) were associated with coarse mode particles such as sodium nitrate and soil, and the coarse mode fraction of total volume concentrations. Although NaNO_3 and soil concentrations were derived from $\text{PM}_{2.5}$ measurements, they are most likely associated with the tail of the coarse mode (Lee et al., 2004). Loadings also suggested that Ångström exponents were anti-correlated with these species as would be expected with the weak spectral dependence of coarse mode particles. As Fig. 2 shows, α_{sfc} and α_{col} decreased around DOY 201, 207, 215–216 and 227. These days were

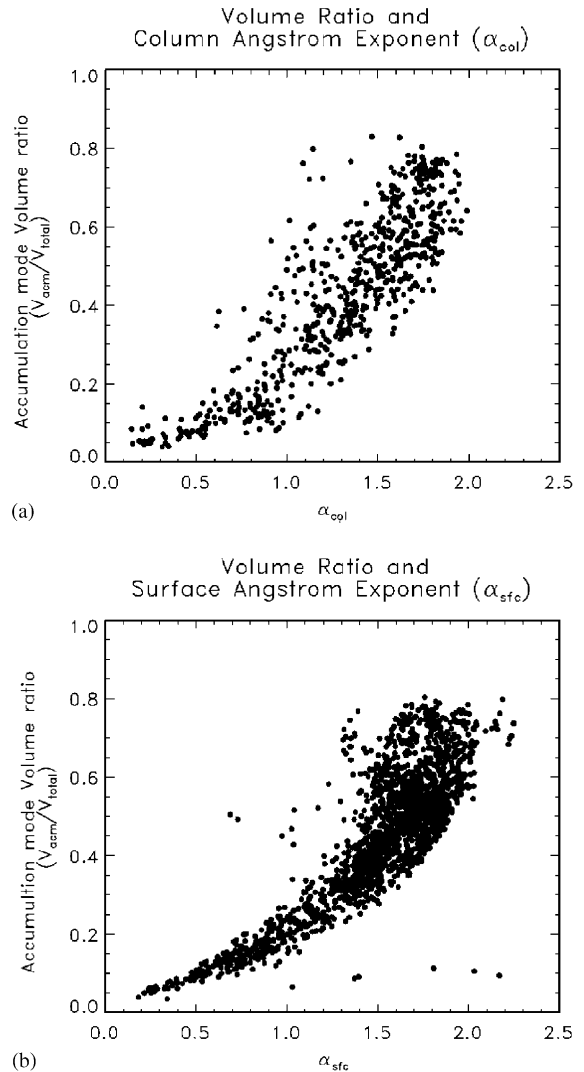


Fig. 3. (a) Ratio of accumulation mode volume concentration to total volume concentration ($V_{\text{acm}}/V_{\text{total}}$) compared to estimates of column (USDA) Ångström exponents. (b) Same as part (a) except for surface estimates of Ångström exponents. Total volume concentrations include accumulation mode, coarse mode and giant mode concentrations.

associated with suspected transport of Saharan dust to the park and corresponded to larger contributions of coarse particles and higher percentages of fine soil in the chemical compositions (Alharbi, 2003; Hand et al., 2002). TOMS aerosol indices (Herman et al., 1999) suggested that Saharan dust transport occurred during the BRAVO study, and synoptic maps also confirmed that several of these transport patterns existed during the early part of the study. Aerosol mineralogical ratios also suggested influences from Saharan regions during this time (Alharbi, 2003; Perry et al., 1997; Sokolik and

Toon, 1999). These transport patterns that are associated with Saharan dust are also likely related to the presence of sodium nitrate because of the influence of sea salt from the Gulf of Mexico. The scores for factor 2 are highest for days in July and early August, as well as days later in October (DOY 281, 290 and 303) that are associated with more local dust sources, increased coarse particle mass and transport from the north (Alharbi, 2003; Hand et al., 2002). The monthly average value of the Ångström exponent was lowest in July, with $\alpha_{\text{sf}} = 1.0 \pm 0.4$ and $\alpha_{\text{col}} = 0.9 \pm 0.4$. Kusmierczyk-Michulec et al. (2002) also found relationships between aerosol mass concentrations and Ångström parameters from measurements on the Baltic Sea. In particular, sea salt mass fractions were found to increase with smaller Ångström parameters, consistent with the negative correlations found in this study for coarse particle composition.

5. Summary

High correlations were observed between surface ambient b_{ext} and remotely sensed τ_{aer} , suggesting that in general the aerosols were well-mixed over the study region and that column τ_{aer} was a good indicator of surface visibility during the BRAVO study. In addition, periods with the highest τ_{aer} and b_{ext} corresponded to aerosols dominated by accumulation mode sulfate as determined by the surface composition and size data. Factor analysis also suggested that ammoniated sulfate contributed significantly to visibility degradation and aerosol column loading. Local effects on aerosol properties due to the different site locations could have affected the comparisons in the two methods, including differences in the vertical distribution of aerosols and altitudinal differences in RH.

Ångström exponents computed for both methods were highly correlated for the majority of the study and on average agreed within experimental uncertainty. Variations in Ångström exponents were consistent with changes in surface aerosol data, with low values observed during periods with suspected Saharan dust influence when coarse mode aerosol and fine soil concentrations were significant. Higher Ångström exponents were observed during periods when aerosol volume concentrations were dominated by accumulation mode particles and sulfate dominated the fine aerosol composition.

Alexandrov et al. (2002) demonstrated the climatological applications of estimating aerosol optical depths from ground-based MFRSR measurements for many sites around the US, and the results in this paper suggest that the USDA UVB network could be very useful for providing continuous estimates of aerosol optical properties for numerous sites around the US. In

addition, we have seen that during the BRAVO study, estimates of aerosol properties from the radiometer were consistent with optical, chemical and physical aerosol properties measured at the surface.

Acknowledgments

Air Resource Specialists are gratefully acknowledged for their logistical efforts during the BRAVO study. T. Lee and J. Collett, Jr. kindly provided composition data. We thank Bill Durham and George Janson for operating the UVB site, and Becky Olson for UVB database management. Support for BRAVO-related work was provided by the National Park Service under Grant CA238099001. However, the results, findings and conclusions expressed in this paper are solely those of the authors and are not necessarily endorsed by the management, sponsors, or collaborators of the BRAVO study. An anonymous reviewer offered helpful suggestions and comments.

References

- Alexandrov, M.D., Laci, A.A., Carlson, B.E., Cairns, B., 2002. Remote sensing of atmospheric aerosols and trace gases by means of multifilter rotating shadowband radiometer. Part II: climatological applications. *Journal of the Atmospheric Sciences* 59, 544–566.
- Alharbi, B.H., 2003. Transport of North African dust to Big Bend, Texas, during the 1999 Big Bend Regional Aerosol and Visibility Observational Study. Masters Thesis, Colorado State University, Colorado.
- Andreae, T.W., Andreae, M.O., Ichoku, C., Maenhaut, W., Cafmeyer, J., Karnieli, A., Orlovsky, L., 2002. Light scattering by dust and anthropogenic aerosol at a remote sensing site in the Negev desert, Israel. *Journal of Geophysical Research* 107 (D2), 10.1029/2001JD900252.
- Andrews, E., Sheridan, P.J., Ogren, J.A., Ferrare, R., 2004. In situ aerosol profiles over the Southern Great Plains cloud and radiation test bed site: 1. Aerosol optical properties. *Journal of Geophysical Research* 109, D06208.
- Ångström, A., 1929. On the atmospheric transmission of Sun radiation and on dust in the air. *Geografiska Annal* 12, 130–159.
- Bergin, M.H., Schwartz, S.E., Halthore, R.N., Ogren, J.A., Hlavka, D.L., 2000. Comparison of aerosol optical depth inferred from surface measurements with that determined by Sun photometry for cloud-free conditions at a continental US site. *Journal of Geophysical Research* 105, 6807–6816.
- Bigelow, D.S., Slusser, J.R., Beaubein, A.F., Gibson, J.H., 1998. The USDA Ultraviolet Radiation Monitoring Program. *Bulletin of the American Meteorological Society* 79, 601–615.
- Charlson, R.J., Schwartz, S.E., Hales, J.M., Cess, R.D., Coakley, J.A., Hansen, J.R., Hofmann, D.J., 1992.

- Climate forcing by anthropogenic aerosols. *Science* 255, 423–430.
- Chow, J.C., Watson, J.G., Pritchett, L.C., Pierson, W.R., Frazier, C.A., Purcell, R.G., 1993. The DRI thermal/optical reflectance carbon analysis system: description, evaluation, and application in US air quality studies. *Atmospheric Environment* 27A (8), 1185–1201.
- Corbin, K.C., Kreidenweis, S.M., Vonder Haar, T.H., 2002. Comparison of aerosol properties derived from Sun photometer data and ground-based chemical measurements. *Geophysical Research Letters* 29(10), 10.1029/2001GL014105.
- Eck, T.F., Holben, B.N., Reid, J.S., Dubovik, O., Smirnov, A., O'Neill, N.T., Slutsker, I., Kinne, S., 1999. Wavelength dependence of the optical depth of biomass burning, urban, and desert dust aerosol. *Journal of Geophysical Research* 104, 31,333–31,349.
- Gebhart, K.G., Kreidenweis, S.M., Malm, W.C., 2001. Back-trajectory analyses of fine particulate matter measured at Big Bend National Park in the historical database and the 1996 scoping study. *Science of the Total Environment* 276, 185–204.
- Hand, J.L., Kreidenweis, S.M., 2002. A new method for retrieving particle refractive index and effective density from aerosol size distributions data. *Aerosol Science and Technology* 36 (10), 1012–1026.
- Hand, J.L., Ames, R.B., Kreidenweis, S.M., Day, D.E., Malm, W.C., 2000. Estimates of particle hygroscopicity during the Southeastern Aerosol and Visibility Study (SEAVS). *Journal of the Air and Waste Management Association* 50, 677–685.
- Hand, J.L., Kreidenweis, S.M., Sherman, D.E., Collett Jr., J.L., Hering, S.V., Day, D.E., Malm, W.C., 2002. Aerosol size distributions during the Big Bend Regional Aerosol Visibility and Observational Study (BRAVO). *Atmospheric Environment* 36, 5043–5055.
- Hansen, J.E., Travis, L.D., 1974. Light scattering in planetary atmospheres. *Space Science Review* 16, 527–610.
- Harrison, L., Michalsky, J., 1994. Objective algorithms for the retrieval of optical depth from ground-based measurements. *Applied Optics* 33, 5126–5132.
- Harrison, L., Michalsky, J., Berndt, J., 1994. Automated multifilter rotating shadow-band radiometer: an instrument for optical depth and radiation measurements. *Applied Optics* 33, 5118–5125.
- Hasan, H., Dzubay, T.G., 1983. Apportioning light extinction coefficients to chemical species in atmospheric aerosol. *Atmospheric Environment* 17 (8), 1573–1581.
- Haywood, J., Boucher, O., 2000. Estimates of the direct and indirect radiative forcing due to tropospheric aerosols: a review. *Review of Geophysics* 38, 513–543.
- Henry, R.C., Hidy, G.M., 1979. Multivariate analysis of particulate sulfate and other air quality variables by principal components—Part I. Annual data from Los Angeles and New York. *Atmospheric Environment* 13, 1581–1596.
- Hering, S.V., Stolzenburg, M.R., Hand, J.L., Kreidenweis, S.M., Lee, T., Collett, J.L., Dietrich, D., Tigges, M., 2003. Hourly concentrations and light scattering cross sections for fine particle sulfate at Big Bend National Park. *Atmospheric Environment* 37, 1175–1183.
- Herman, J.R., Krotkov, N., Celarier, E., Larko, D., Labow, G., 1999. Distribution of UV radiation at the Earth's surface from TOMS-measured UV-backscattered radiances. *Journal of Geophysical Research* 104, 12,059–12,076.
- Holben, B.N., Eck, T.F., Slutsker, I., Tanre, D., Buis, J.P., Setzer, A., Vermote, E., Reagan, J.A., Kaufman, Y.J., Nakajima, T., Lavenu, F., Jankowiak, I., Smirnov, A., 1998. AERONET—a federated instrument network for aerosol characterization. *Remote Sensing of Environment* 66, 1–16.
- Intergovernmental Panel on Climate Change (IPCC), 2001. Climate contribution of Working Group I to the third assessment report of the Intergovernmental Panel on Climate Change, 2001. In: Houghton, J.T., Ding, Y., Griggs, D.J., Noguer, M., van der Linden, P.M., Dai, X., Maskell, K., Johnson, C.A. (Eds.), *Change 2001: The Scientific Basis*. Cambridge University Press, Cambridge, UK and New York, NY, USA, 881pp.
- Kato, S., Bergin, M.H., Ackerman, T.P., Charlock, T.P., Clothiaux, E.E., Ferrare, R.A., Halthore, R.N., Laulainen, N., Mace, G.G., Michalsky, J., Turner, D.D., 2000. A comparison of the aerosol thickness derived from ground-based and airborne measurements. *Journal of Geophysical Research* 105, 14,701–14,717.
- Kusmierczyk-Michulec, J., de Leeuw, G., Robles Gonzalez, C., 2002. Empirical relationships between aerosol mass concentrations and Ångström parameter. *Geophysical Research Letters* 29, 10.1029/2001GL014128.
- Lee, T., Kreidenweis, S.M., Collett Jr., J.L., 2004. Aerosol ion characteristics during the Big Bend Regional Aerosol and Visibility Observational Study. *Journal of the Air and Waste Management Association* 54, 585–592.
- Malm, W.C., Kreidenweis, S.M., 1997. The effects of models of aerosol hygroscopicity on the apportionment of extinction. *Atmospheric Environment* 31 (13), 1965–1976.
- Malm, W.C., Sisler, J.F., Huffman, D., Eldred, R.A., Cahill, T.A., 1994. Spatial and seasonal trends in particle concentration and optical extinction in the United States. *Journal of Geophysical Research* 99, 1347–1370.
- Malm, W.C., Day, D.E., Kreidenweis, S.M., Collett, J.L., Lee, T., 2003. Humidity-dependent optical properties of fine particles during the Big Bend Regional Aerosol and Visibility Observational Study. *Journal of Geophysical Research* 108 (D9), 4279.
- McArthur, L.J.B., Halliwell, D.H., Niebergall, O.J., O'Neill, N.T., Slusser, J.R., Wehrli, C., 2003. Field comparison of network Sun photometers. *Journal of Geophysical Research* 108 (D19), 4596.
- Nakajima, T., Higurashi, A., 1998. A use of two-channel radiances for an aerosol characterization from space. *Geophysical Research Letters* 25, 3815–3818.
- Ouimette, J.R., Flagan, R.C., 1982. The extinction coefficient of multi-component aerosols. *Atmospheric Environment* 16 (10), 2405–2419.
- Perry, K.D., Cahill, T.A., Eldred, R.A., Dutcher, D.D., 1997. Long-range transport of North African dust to the eastern United States. *Journal of Geophysical Research* 102, 11,225–11,238.
- Reid, J.S., Eck, T.F., Christopher, S.A., Hobbs, P.V., Holben, B., 1999. Use of the Ångström exponent to estimate the variability of optical and physical properties of aging smoke

- particles in Brazil. *Journal of Geophysical Research* 104, 27,473–27,489.
- Schmid, B., Michalsky, J., Halthore, R., Beauharnois, M., Harrison, L., Livingston, L., Russell, P., Holben, B., Eck, T., Smirnov, A., 1999. Comparison of aerosol optical depth from four solar radiometers during the fall of 1997 ARM intensive observation period. *Geophysical Research Letters* 26, 2725–2728.
- Slusser, J., Gibson, J., Bigelow, D., Kolinski, D., Disterhoft, P., Lantz, K., Beaubien, A., 2000. Langley method for calibrating UV filter radiometers. *Journal of Geophysical Research* 105, 4841–4849.
- Smirnov, A., Holben, B.N., Slutsker, I., Welton, E.J., Formenti, P., 1998. Optical properties of Saharan dust during ACE 2. *Journal of Geophysical Research* 103, 28,079–28,092.
- Smirnov, A., Holben, B.N., Eck, T.F., Dubovik, O., Slutsker, I., 2000. Cloud screening and quality control algorithms for the AERONET database. *Remote Sensing of Environment* 73, 337–349.
- Sokolik, I.N., Toon, O.B., 1999. Incorporation of mineralogical composition into models of the radiative properties of mineral aerosol from UV to IR wavelengths. *Journal of Geophysical Research* 104, 9423–9444.
- Tang, I.N., 1996. Chemical and size effects of hygroscopic aerosols on light scattering coefficients. *Journal of Geophysical Research* 101, 19,245–19,250.